The split majoron model confronts the NANOGrav signal

Pasquale Di Bari, and Moinul Hossain Rahat

School of Physics and Astronomy, University of Southampton, Southampton, SO17 1BJ, U.K.

Abstract: In the light of the evidence of a gravitational wave background from the NANOGrav 15yr data set, we reconsider the split majoron model as a new physics extension of the standard model able to generate a needed contribution to solve the current tension between the data and the standard interpretation in terms of inspiraling supermassive black hole massive binaries. In the split majoron model the seesaw right-handed neutrinos acquire Majorana masses from spontaneous symmetry breaking of global $U(1)_{B-L}$ in a strong first order phase transition of a complex scalar field occurring above the electroweak scale. The final vacuum expectation value couples to a second complex scalar field undergoing a low scale phase transition occurring after neutrino decoupling. Such a coupling enhances the strength of this second low scale first order phase transition and can generate a sizeable primordial gravitational wave background contributing to the NANOGrav 15yr signal. Moreover, the free streaming length of light neutrinos can be suppressed by their interactions with the resulting Majoron background and this can mildly ameliorate existing cosmological tensions, thus providing a completely independent motivation for the model.

Contents

1 Introduction 1

2 The split majoron model 2

3 Cosmological constraints 3

4 GW spectrum predictions confronting the NANOGrav signal 6

5 Final remarks 10

1 Introduction

The NANOGrav collaboration has found evidence for a gravitational wave (GW) background at $\sim$ nHZ frequencies in the 15-year data set [1–4]. This strongly relies on the observed correlations among 67 pulsars following an expected Hellings-Downs pattern for a stochastic GW background [5]. A simple baseline model is provided by a standard interpretation in terms of inspiraling black hole binaries (SMBHBs) with a fiducial $f^{-2/3}$ characteristic strain spectrum. Such a baseline model provides a poor fit to the data and some deviation is currently favoured. In particular, models where in addition to SMBHBs one also has a contribution from new physics provide a better fit of the NANOGrav data than the baseline model, resulting in Bayes factors between 10 and 100 [4][1].

First order phase transitions at low scales can provide such an additional contribution. For temperatures of the phase transition in the range 1 MeV – 1 GeV, the resulting GW background can explain the entire NANOGrav signal [4]. However, when a realistic model is considered, one needs also to take into account the cosmological constraints on the amount of extra radiation from big bang nucleosynthesis (BBN) and CMB anisotropies. A phase transition associated to the spontaneous breaking of a $U(1)_{L_I}$ symmetry, where a Majorana mass term is generated, has been previously discussed [64] as a potential origin for the NANOGrav signal from 12.5-year data set [2, 3]. In this case a complex scalar field gets a non-vanishing vacuum expectation value at the end of the phase transition and a right-handed neutrino, typically the lightest, coupling to it acquires a Majorana mass. The phase transition involves only a few additional degrees of freedom forming a dark sector, and some of them can decay into ordinary neutrinos potentially producing extra radiation so that cosmological constraints need to be considered. It has been shown that these can be respected if the phase transition occurs after neutrino decoupling since in this case the dark sector thermalises only with decoupled ordinary neutrinos and the amount of extra radiation does not exceed upper bounds from big bang nucleosynthesis and CMB

[1] see Refs. [6–63] for some recent new physics approaches.

temperature anisotropies. In [64] it was concluded that the amplitude of the NANOGrav signal was too high to be explained by such a phase transition since the peak of the predicted spectrum was two order of magnitudes below the signal. This conclusion was based on 12.5-year data and on a way to calculate the sound wave contribution to the GW spectrum valid for values of the strength of the phase transition $\alpha \lesssim 0.1$ that is now outdated [65]. In this paper we reexamine this conclusion in the light of the 15 year data set and adopting an improved description of the sound wave contribution, applicable for larger values of α. We confirm that such a phase transition can hardly reproduce the whole signal but can well be combined to the contribution from the SMBHBs baseline model to improve the fit of the signal.

The paper is structured as follows. In Section 2 we discuss the split Majoron model. In Section 3 we discuss the cosmological constraints deriving by the presence of extra radiation in the model. In Section 4 we review the calculation of the GW spectrum and show the results we obtain and compare them to the NANOGrav 15 year-data set. In Section 5 we draw our conclusions and discuss future developments .

2 The split majoron model

We discuss now a model that was sketched in [64] and that can be regarded as an extension of the multiple majoron model proposed in [66]. Compared to the traditional majoron model [67], we have two complex scalar fields each undergoing its own first order phase transition, one at high scale, above the electroweak scale, and one at much lower scale, dictated by the possibility to address the NANOGrav signal. If we denote by ϕ and ϕ' the two complex scalar fields, respectively, we can write the Lagrangian as ($I = 1, \dots, N$ and $I' = N, \dots, N + N'$):

$$\begin{aligned} -\mathcal{L}_{N_I+N_{I'}+\phi+\phi'} = {} & \overline{L_\alpha}\, h_{\alpha I}\, N_I\, \widetilde{\Phi} + \frac{\lambda_I}{2}\, \phi\, \overline{N_I^c}\, N_I \\ & + \overline{L_\alpha}\, h_{\alpha I'}\, N_{I'}\, \widetilde{\Phi} + \frac{\lambda_{I'}}{2}\, \phi'\, \overline{N_{I'}^c}\, N_{I'} + V_0(\phi, \phi') + \text{h.c.}\,, \end{aligned} \tag{2.1}$$

where Φ is the SM Higgs doublet and $\widetilde{\Phi}$ its dual and the $N_I, N_{I'}$ are the RH neutrinos coupling to ϕ, ϕ'. Imposing that the Lagrangian (2.1) obeys a $U(1)_{\sum_I L_I} \times U(1)_{\sum_I' L_I'}$ symmetry, we can take as (renormalisable) tree level potential (with no $\phi - \Phi$ and $\phi' - \Phi$ couplings)

$$V_0(\phi, \phi') = -\mu^2\, |\phi|^2 + \lambda\, |\phi|^4 - \mu'^2 |\phi'|^2 + \lambda' |\phi'|^4 + \zeta |\phi|^2\, |\phi'|^2\,. \tag{2.2}$$

We will assume that ϕ undergoes a phase transition, breaking a $U(1)_{L_1+\dots+L_N}$ global symmetry, at some scale above the electroweak scale. In the broken phase we can rewrite ϕ as

$$\phi = \frac{e^{i\theta}}{\sqrt{2}}\, (v_0 + S + i\, J)\;, \tag{2.3}$$

where v_0 is the ϕ vacuum expectation value, S is a massive boson field with mass $m_S = \sqrt{2\lambda}\, v_0$ and J is a Majoron, a massless Goldstone field. The vacuum expectation value of ϕ generates RH neutrino masses $M_I = \lambda_I\, v_0/\sqrt{2}$. After electroweak symmetry breaking, the vacuum expectation value of the Higgs generates Dirac neutrino masses $m_{D\alpha I} = v_{\rm ew}\, h_{\alpha I}/\sqrt{2}$ and $m_{D\alpha I'} = v_{\rm ew}\, h_{\alpha I'}/\sqrt{2}$, where $v_{\rm ew} = 246\,{\rm GeV}$ is the standard Higgs vacuum expectation value. In the case of the RH neutrinos N_I, their Majorana masse lead, via type-I seesaw mechanism, to a light neutrino mass matrix given by the seesaw formula,

$$(m_\nu)_{\alpha\beta} = -\frac{v_{\rm ew}^2}{2}\,\frac{h_{\alpha I} h_{\beta I}}{M_I}\,, \tag{2.4}$$

Notice that we are writing the neutrino Yukawa matrices in the flavour basis where both charged leptons and Majorana mass matrices are diagonal. The Yukawa couplings $h_{\alpha I'}$ have to be taken much smaller than usual massive fermions Yukawa couplings or even vanishing, as we will point out.

Eventually, at a lower scale, much below the electroweak scale, ϕ' also undergoes a first order phase transition breaking the $U(1)_{L_{1'}+\dots+L_{N'}}$ symmetry. In the broken phase we can rewrite ϕ' as

$$\phi' = \frac{e^{i\theta}}{\sqrt{2}}\,\left(v_0' + S' + i\,J'\right)\,, \tag{2.5}$$

where v_0' is the ϕ vacuum expectation value and again S' is a massive boson field with mass $m_{S'} = \sqrt{2\lambda'}\,v_0'$ and J' is a massless Majoron. The vacuum expectation value of ϕ' generates RH neutrino masses $M_{I'} = \lambda_{I'}\,v_0'/\sqrt{2}$.

Let us now draw two different cases we will consider. We have a minimal case with $N = 2$ and $N' = 1$. In this case one would have that the seesaw formula generates the atmospheric and solar neutrino mass scales while the lightest neutrino would be massless. However, after the electroweak symmetry breaking and before the ϕ' phase transition, the small Yukawa couplings $h_{\alpha 3}$ generate a small Dirac neutrino mass for the lightest neutrino in a way to have an hybrid case where two neutrino mass eigenstates are Majorana neutrinos and the lightest is a Dirac neutrino. Finally, at the ϕ' phase transition a Majorana mass M_3 is generated and one has a second seesaw giving a lightest neutrino mass $m_1 = \sum_\alpha |m_{D\alpha 3}|^2/M_3$.[2]

In a second case one has $N = 3$ and a generic N'. In this case the Yukawa couplings $h_{\alpha I'}$ can even vanish. The RH neutrinos $N_{I'}$ acquire a Majorana mass at the ϕ' phase transition but they do not contribute to the ordinary neutrino masses. They can be regarded as massive neutral leptons in the dark sector, with no interactions with the visible sector (including the seesaw neutrinos).

As we will be better explain in Section 4, the vacuum expectation value of the complex scalar field ϕ will increase the strength of the ϕ' phase transition and this will be crucial in enhancing the amplitude of the generated GW spectrum.

3 Cosmological constraints

Let us now consider the impact on the model of cosmological constraints on the amount of extra-radiation coming from big bang nucleosynthesis and CMB anisotropies. Let us first of all calculate the evolution of the number of degrees of freedom in the model.

[2] Notice that N_3 is the lightest RH neutrino and not the heaviest.

The number of energy density ultra-relativistic degrees of freedom $g_\rho(T)$ is defined as usual by $\rho_R(T) \equiv g_\rho(T)(\pi^2/30)\, T^4$, where $\rho_R(T)$ is the energy density in radiation. In our case it receives contributions from the SM sector and from the dark sector, so that we can write $g_\rho(T) = g_\rho^{\rm SM}(T) + g_\rho^{\rm dark}(T)$. At the ϕ phase transition, occurring at a phase transition temperature $T_\star$ above the electroweak scale, one has for the SM contribution $g_\rho^{\rm SM}(T_\star) = 106.75$ and for the dark sector contribution

$$g_\rho^{\rm dark}(T_\star) = g_\rho^{J+S} + \frac{7}{4}\, N \,, \tag{3.1}$$

where $g_\rho^{J+S} = 2$. Notice here we are assuming the N seesaw neutrinos all thermalise at the phase transition. This is something that can always be realised since all their decay parameters, defined as $K_I \equiv (h^\dagger\, h)_{II}\, \bar{v}_{\rm ew}^2/(M_I\, m_{\rm eq})$ with the effective equilibrium neutrino mass $m_{\rm eq} = [16\pi^{5/2}\sqrt{g_\rho^\star}/(3\sqrt{5})]\,(v_{\rm eq}/M_{\rm P})$ and $\bar{v}_{\rm ew} = v_{\rm ew}/\sqrt{2} = 174\,{\rm GeV}$, can be larger than unity in agreement with neutrino oscillation experiments. Therefore, at the high scale phase transition the dark sector is in thermal equilibrium with the SM sector thanks to the seesaw neutrino Yukawa couplings.

After the phase transition all massive particles in the dark sector, S plus the N seesaw neutrinos will quickly decay, while the massless majoron J will contribute to extra radiation. We can then track the evolution of $g_\rho(T)$ at temperatures below $T_\star$ and prior to the low scale phase transition occurring at a temperature $T'_\star$ and also prior to any potential process of *rethermalisation* of the dark sector that we will discuss later.

In particular, we can focus on temperatures $T \ll m_\mu \sim 100\,{\rm MeV}$. In this case the SM contribution can be written as [68]

$$g_\rho^{\rm SM}(T \ll 100\,{\rm MeV}) = g_\varepsilon^{\gamma+e^\pm+3\nu}(T) = 2 + \frac{7}{8}\,\left[4\, g_\varepsilon^e(T) + 6\, r_\nu^4(T)\right]\,, \tag{3.2}$$

where the number of energy density ultra-relativistic degrees of freedom of electrons per single spin degree is given by

$$g_\rho^e(T) = \frac{90}{7\,\pi^4}\int_0^\infty dx\, \frac{x^2\,\sqrt{x^2+z^2}}{e^{\sqrt{x^2+z^2}}+1}\,, \tag{3.3}$$

where $z \equiv m_e/T$. Above the electron mass one has $g_\rho^e(T \gg m_e) = 1$, while of course $g_\rho^e(T) \to 0$ for $T/m_e \to 0$. The neutrino-to-photon temperature ratio $r_\nu(T) \equiv T_\nu(T)/T$ can be as usual calculated using entropy conservation,

$$r_\nu(T) = \left(\frac{2}{11}\right)^{\frac{1}{3}}\,\left[g_s^{\gamma+e^\pm}(T)\right]^{\frac{1}{3}}\,, \tag{3.4}$$

where

$$g_s^{\gamma+e^\pm}(T) = 2 + \frac{7}{2}\, g_s^e(T)\,, \tag{3.5}$$

having defined the contribution to the number of entropy density ultra-relativistic degrees of freedom of electrons per single spin degree given by

$$g_s^e(T) = \frac{8}{7}\frac{45}{4\pi^4}\int_0^\infty dx\, \frac{x^2\,\sqrt{x^2+z^2}+\frac{1}{3}\,\frac{x^4}{\sqrt{x^2+z^2}}}{e^{\sqrt{x^2+z^2}}+1}\,. \tag{3.6}$$

where $z \equiv m_e/T$. One can again verify that $g_s^e(T \gg m_e) = 1$ and $g_s^e(T) \to 0$ for $T/m_e \to 0$ so that one recovers the well known result $r_\nu(T \ll m_e) = (4/11)^{1/3}$. With this function one can write the SM number of entropy density ultra-relativistic degrees of freedom as

$$g_s^{\rm SM}(T \ll m_\mu) = g_s^{\gamma+e^\pm+3\nu}(T) = 2 + \frac{7}{8}\left[4\, g_s^e(T) + 6\, r_\nu^3(T)\right] . \tag{3.7}$$

For $T \ll m_e$ one recovers the well known result $g_s^{\rm SM}(T \ll m_e) = 43/11 \simeq 3.91$ and $g_\rho^{\rm SM}(T \ll m_e) \simeq 3.36$. Let us now focus on the dark sector contribution. This is very easy to calculate since one has simply $g_\rho^{\rm dark}(T) = g_J\,[r_{\rm dark}(T)]^4$, where $g_J = 1$ and where the dark sector-to-photon temperature ratio can be again calculated from entropy conservation as

$$r_{\rm dark}(T) = \left[\frac{g_s^{\rm SM}(T)}{g_s^{\rm SM}(T_\star)}\right]^{1/3} . \tag{3.8}$$

For example, for $m_\mu \gg T \gg m_e$ one finds $r_{\rm dark}(T) = (43/427)^{1/3} \simeq 0.465$. We can also rewrite $g_\rho^{\rm dark}(T)$ in terms of the extra-effective number of neutrino species $\Delta N_\nu(T)$ defined as

$$g_\rho^{\rm dark}(T) = \frac{7}{4}\,\Delta N_\nu^{\rm eff}\,[r_\nu(T)]^4 . \tag{3.9}$$

For example, at $m_\mu \gg T \gg m_e$ one finds

$$\Delta N_\nu^{\rm eff}(T) = \frac{4}{7}\,g_J\,[r_{\rm dark}(T)]^4 = \frac{4 \times 43}{7 \times 427}^{\frac{4}{3}} \simeq 0.05 . \tag{3.10}$$

Such a small contribution to extra radiation is in agreement with all cosmological constraints that we can summarise as:

- From primordial helium-4 abundance measurements combined with the baryon abundance extracted from cosmic microwave background (CMB) anisotropies placing a constraint on $\Delta N_\nu^{\rm eff}(t)$ at $t = t_{\rm f} \sim 1\,{\rm s}$, the time of freeze-out of the neutron-to-proton ratio [69]:

$$\Delta N_\nu^{\rm eff}(t_{\rm f}) \simeq -0.1 \pm 0.3 \;\Rightarrow\; \Delta N_\nu^{\rm eff}(t_{\rm f}) \lesssim 0.5 \quad (95\%\,{\rm C.L.}) . \tag{3.11}$$

- From measurements of the primordial deuterium abundance at the time of nucleosynthesis, $t_{\rm nuc} \simeq 310\,{\rm s}$, corresponding to $T_{\rm nuc} \simeq 65\,{\rm keV}$ [68]:

$$\Delta N_\nu^{\rm eff}(t_{\rm nuc}) = -0.2 \pm 0.3 \;\Rightarrow\; \Delta N_\nu^{\rm eff}(t_{\rm nuc}) \lesssim 0.4 \quad (95\%\,{\rm C.L.}) . \tag{3.12}$$

- From CMB temperature and polarization anisotropies constrain $\Delta N_\nu^{\rm eff}(t)$ at recombination, when $T \simeq T_{\rm rec} \simeq 0.3\,{\rm eV}$, and the *Planck* collaboration finds [70]

$$\Delta N_\nu^{\rm eff}(t_{\rm rec}) = -0.06 \pm 0.17 \;\Rightarrow\; \Delta N_\nu^{\rm eff}(t_{\rm rec}) \lesssim 0.3 \quad (95\%\,{\rm C.L.}) . \tag{3.13}$$

Let us now consider the low scale phase transition, assuming this occurs at a temperature $T'_\star$ above neutrino decoupling, so that $r_\nu(T'_\star) = 1$. At such low temperatures, below 1 GeV, Yukawa couplings are ineffective to rethermalise the dark sector [64]. Therefore, at the phase transition, the dark sector will have a temperature $T'_{\mathrm{dark},\star} \simeq 0.465\, T'_\star$ and with such a small temperature one would obtain a GW production much below the NANOGrav signal. Notice that after the phase transition the second majoron J' would contribute to dark radiation with a contribution to $\Delta N_\nu(T)$ equivalent to the contribution from J in a way that $\Delta N_\nu(T) \simeq 0.1$.

One could envisage some interaction able to rethermalise the dark sector so that $r_{\mathrm{dark}}(T'_{\mathrm{dark},\star} = 1$. However, in this case one would have that the J' abundance would yield $\Delta N_\nu(T) \simeq 8/14 \simeq 0.6$ throughout BBN and recombination, in disagreement with the cosmological constraints we just reviewed.[3] For this reason we now consider, as in [64], the case when the phase transitions occurs below neutrino decoupling ($T'_\star \lesssim 1\,\mathrm{MeV}$).

In this case a rethermalisation can occur between the dark sector and just the decoupled ordinary neutrino background. Prior to the ϕ' phase transition one has the interactions

$$-\mathcal{L}_{\nu-\mathrm{dark}} = \frac{i}{2} \sum_{i=2,3} \lambda_i\, \overline{\nu_i}\, \gamma^5\, \nu_i\, J \tag{3.14}$$

that can thermalise the majoron J with the ordinary neutrinos and via the coupling $\zeta J |\phi'|^2$ also the complex scalar field ϕ'. In this way ordinary neutrinos would loose part of their energy that is transferred to the dark sector in a way that they reach a common temperature such that [71–73]

$$r_T = \left(\frac{4}{11}\right)^{\frac{1}{3}} \left(\frac{3.044}{3.044 + N' + 12/7}\right)^{\frac{1}{4}} . \tag{3.15}$$

For $N' = 1$ one finds $r_T \simeq 0.6$. One also has some extra radiation equivalent to

$$\Delta N_\nu^{\mathrm{eff}} \simeq 3.044 \left(\frac{3.044 + N' + 12/7}{3.044 + N' + 12/7 - N_{\mathrm{h}}}\right)^{\frac{1}{3}} - 3.044 \simeq 0.5\,, \tag{3.16}$$

where N_{h} is the number of massive states that after the phase transition decay and produce the excess radiation. In our case these states are given by S' and the N' RH neutrinos so that $N_h = N' + 1$. For $N' = 1$ one gets $\Delta N_\nu^{\mathrm{eff}} \simeq 0.5$. This model can also ameliorate the Hubble tension [72, 74] compared to the ΛCDM model since one has a simultaneous injection of extra radiation together with a reduction of the neutrino free streaming length due to the interactions between the ordinary neutrinos and the majorons. Recently a new analysis of this model has been presented in [75] where it has been found that the improvement is more contained than previously found. Still however it is interesting that this model can nicely link the NANOGrav signal, that we are going to discuss in the next section, to the cosmological tensions.

4 GW spectrum predictions confronting the NANOGrav signal

We first briefly review how the first order phase transition parameters relevant for the production of GW spectrum in the split Majoron model are calculated and refer the interested

[3] A possible interesting caveat to this conclusion is to modify the model introducing an explicit symmetry breaking term that would give J' a mass. In this way J' might decay prior to neutron-to-proton freeze out thus circumventing all constraints. We will be back in the final remarks on this possible scenario.

reader to Ref. [66] for a broader discussion. The finite-temperature effective potential for the scalar ϕ' can be calculated perturbatively at one-loop level and is the summation of zero temperature tree-level and one-loop Coleman-Weinberg potential and one-loop thermal potential. Using thermal expansion of the one-loop thermal potential, this can be converted in a *dressed effective potential* given by

$$V_{\rm eff}^{T}(\varphi') \simeq \frac{1}{2}\,\widetilde{M}_T^2\,\varphi'^2 - (A\,T + C)\,\varphi'^3 + \frac{1}{4}\lambda_T\,\varphi'^4\,. \tag{4.1}$$

Here, a zero-temperature cubic term $C = \zeta^2 v_0'/(2\lambda')$ is introduced due to the presence of the scalar ϕ with a high scale vacuum expectation value during the phase transition of ϕ' at a lower scale. This term significantly enhances the strength of the phase transition. The other parameters in Eq. (4.1) are given by

$$\widetilde{M}_T^2 \equiv 2\,D\,(T^2 - T_0^2)\,, \tag{4.2}$$

where the destabilisation temperature T_0 is given by

$$2\,D\,T_0^2 = \lambda'\,v_0'^2 + \frac{N'}{8\,\pi^2}\,\frac{M'^4}{v_0'^2} - \frac{3}{8\,\pi^2}\lambda'^2\,v_0'^2\,, \tag{4.3}$$

and the dimensionless constant coefficients D and A are expressed as

$$D = \frac{\lambda'}{8} + \frac{N'}{24}\,\frac{M'^2}{v_0'^2} \quad \text{and} \quad A = \frac{(3\,\lambda')^{3/2}}{12\pi}\,. \tag{4.4}$$

The dimensionless temperature dependent quartic coefficient λ_T is given by

$$\lambda_T = \lambda' - \frac{N'\,M'^4}{8\,\pi^2\,v_0'^4}\,\log\frac{a_F\,T^2}{e^{3/2}\,M'^2} + \frac{9\lambda^2}{16\pi^2}\,\log\frac{a_B\,T^2}{e^{3/2}\,m_S'^2}\,. \tag{4.5}$$

The cubic term is negligible at very high temperatures and the potential is symmetric with respect to ϕ'. But at lower temperatures it becomes important and a stable second minimum forms at a nonzero ϕ', and bubbles nucleate from the 'false' vacuum to the 'true' vacuum with a nonzero probability. We refer to $T_\star'$ as the characteristic phase transition temperature and identify it with the percolation temperature when $1/e$ fraction of space is still in the false vacuum. Two other parameters relevant for the calculation of GW spectrum from phase transition are α and $\beta/H_\star$, where the first denotes the strength of the phase transition and the latter describes the inverse of the duration of the phase transition. These parameters are defined as

$$\frac{\beta}{H_\star} \simeq T_\star\,\frac{d(S_3/T)}{dT}\bigg|_{T_\star}\,, \qquad \text{and} \qquad \alpha \equiv \frac{\varepsilon(T_\star)}{\rho(T_\star)}\,, \tag{4.6}$$

where S_3 is the spatial Euclidean action, $\varepsilon(T_\star)$ is the latent heat released during the phase transition and $\rho(T_\star)$ is the total energy density of the plasma, including both SM and dark sector degrees of freedom. An approximate analytical estimate for calculating S_3/T and $T_\star'$ in terms of the model parameters can be found in Ref. [66]. In calculating α for phase transition at low temperatures, one must be careful about various cosmological constraints, as outlined in section 3.

We now proceed to calculate the GW spectrum of the model relevant for nanoHZ frequencies. Assuming that first order phase transition occurs in the detonation regime where bubble wall velocity $v_w > c_s = 1/\sqrt{3}$, the dominant contribution to the GW spectrum mainly comes from sound waves in the plasma, and is given by [65, 76, 77]

$$h^2\Omega_{\rm sw0}(f) = 1.45\times 10^{-6}\,\frac{\widetilde{\Omega}_{\rm gw}}{10^{-2}}\,\frac{v_{\rm w}(\alpha)}{\beta/H_\star}\left[\frac{\kappa(\alpha)\,\alpha}{1+\alpha}\right]^2\left(\frac{106.75}{g_\rho^\star}\right)^{1/3} S_{\rm sw}(f)\,\Upsilon(\alpha,\beta/H_\star). \quad (4.7)$$

Here the spectral shape function $S_{\rm sw}(f)$ is given by

$$S_{\rm sw}(f) = \left(\frac{f}{f_{\rm sw}}\right)^3\left[\frac{7}{4+3(f/f_{\rm sw})^2}\right]^{7/2}, \quad (4.8)$$

and the peak frequency $f_{\rm sw}$ can be expressed as

$$f_{\rm sw} = 8.9\,\mu{\rm Hz}\,\frac{1}{v_{\rm w}}\,\frac{\beta}{H_\star}\,\frac{T_\star}{100\,{\rm GeV}}\left(\frac{g_\rho^\star}{106.75}\right)^{1/6}. \quad (4.9)$$

We adopt Jouguet detonation solution for which the efficiency factor is given by [78, 79]

$$\kappa(\alpha) \simeq \frac{\alpha}{0.73+0.083\sqrt{\alpha}+\alpha}, \quad (4.10)$$

and the bubble wall velocity $v_{\rm w}(\alpha) = v_{\rm J}(\alpha)$, where

$$v_{\rm J}(\alpha) \equiv \frac{\sqrt{1/3}+\sqrt{\alpha^2+2\alpha/3}}{1+\alpha}. \quad (4.11)$$

There are two suppression factors in Eq. (4.7). One is the prefactor $\widetilde{\Omega}_{\rm gw} = 10^{-3}$–$10^{-2}$ [80], whose exact value depends on various simulation parameters. We will show the spectrum for $\widetilde{\Omega}_{\rm gw} = 10^{-2}$ with solid/dashed lines below which there is a band covering up to $\widetilde{\Omega}_{\rm gw} = 10^{-3}$ in our GW spectrum plots in Figs. 1 and 2. The other suppression factor $\Upsilon(\alpha,\beta/H_\star) \le 1$ and is given by [81, 82]:

$$\Upsilon(\alpha,\beta/H_\star) = 1-\frac{1}{\sqrt{1+2\,H_\star\tau_{\rm sw}}}, \quad (4.12)$$

where we can write

$$H_\star\tau_{\rm sw} = (8\,\pi)^{\frac{1}{3}}\,\frac{v_{\rm w}}{\beta/H_\star}\left[\frac{1+\alpha}{\kappa(\alpha)\,\alpha}\right]^{1/2}. \quad (4.13)$$

We refer the interested reader to Ref. [66] for a detailed discussion about the known issues and caveats in using the above expressions for calculating GW spectrum. Nevertheless, we show the GW spectrum for a set of benchmark points given in Table 1 and 2 in Figs. 1 and 2, respectively.

The left panel of Fig. 1 shows GW spectra peaked in the frequency range probed by NANOGrav for $N' = 1$. The parameters α and β decreases and increases, respectively, from the benchmark point Ⓐ to Ⓒ, weakening the GW peak amplitude. In Fig. 2, we show two

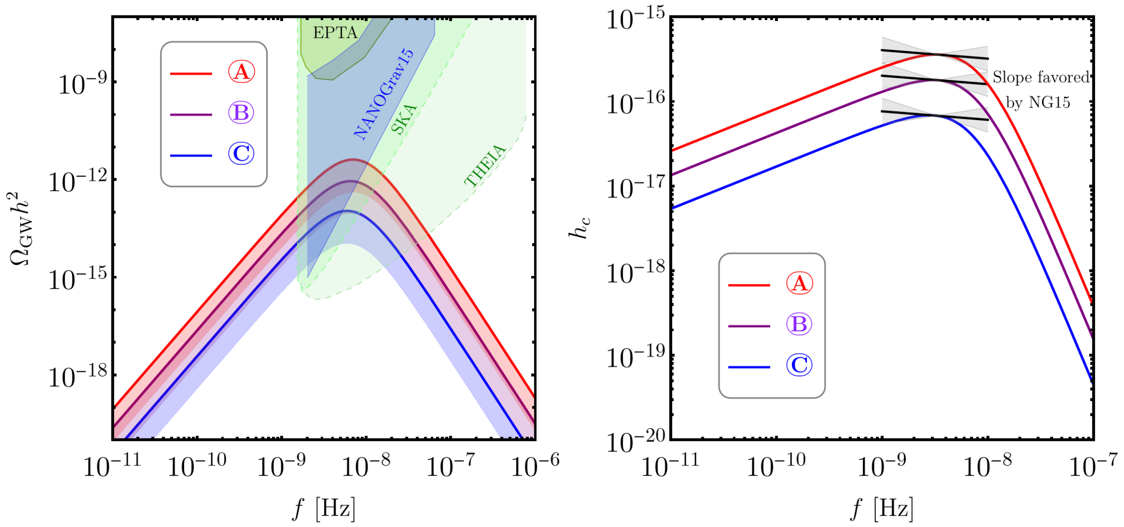

Figure 1. *Left:* GW spectrum at NANOGrav for $N' = 1$ and different α. *Right:* Strain spectrum compared to best fit from NANOGrav 15-yr data. Benchmark points are given in Table 1.

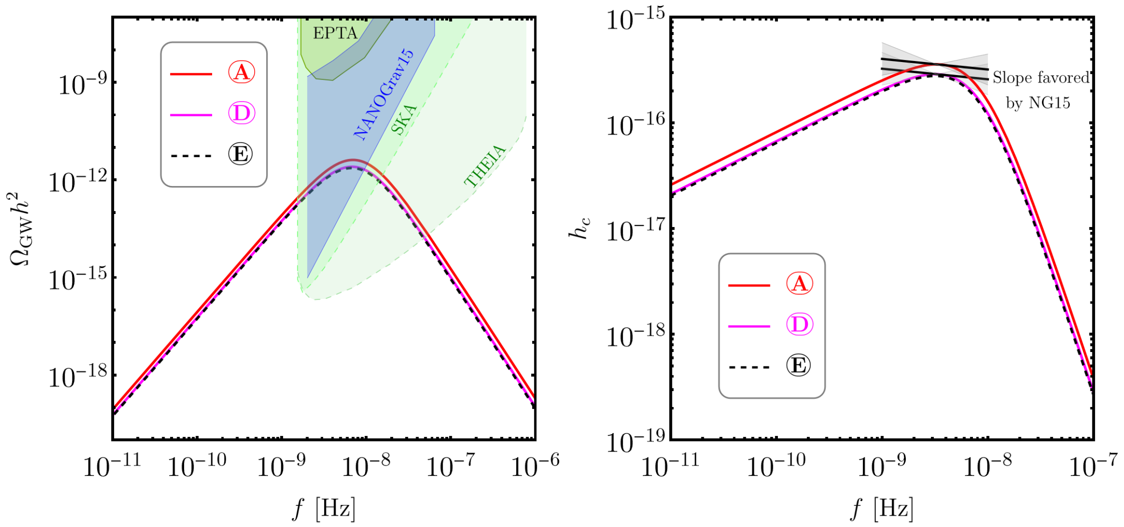

Figure 2. *Left:* GW spectrum at NANOGrav with different N'. *Right:* Strain spectrum compared to best fit from NANOGrav 15-yr data. Benchmark points are given in Table 2.

B.P.	N'	λ'	v_0' [keV]	M' [keV]	C	α	$\beta/H_\star$	$T_\star$ [keV]
Ⓐ	1	0.0023	90.25	33.0	1.85	0.60	432.73	302.53
Ⓑ	1	0.0022	120.25	34.0	0.82	0.40	616.54	192.93
Ⓒ	1	0.0033	83.25	24.6	0.65	0.20	754.02	134.93

Table 1. Benchmark points for GW signals from first order phase transition of ϕ' for $N' = 1$.

B.P.	N'	λ'	v_0' [keV]	M' [keV]	C	α	$\beta/H_\star$	$T_\star$ [keV]
Ⓐ	1	0.0023	90.25	33.0	1.85	0.60	432.73	302.53
Ⓓ	3	0.0031	36.15	7.0	1.45	0.60	548.69	234.5
Ⓔ	5	0.0018	141.4	18.2	0.96	0.60	584.46	220.51

Table 2. Benchmark points for phase transition of ϕ' with different N'.

more benchmark points Ⓓ and Ⓔ which have the same α as the benchmark point Ⓐ, and slightly different $\beta/H_\star$. The resulting spectra is very similar, showing that the maximum GW signal that can be achieved in this model in the NANOGrav frequencies is somewhat independent of N'.

In the right panel of Figs. 1 and 2 we show the dimensionless strain $h_c(f)$ of the GW signals, given by

$$h_c(f) = \sqrt{\frac{2\mathcal{H}_0^2\Omega_{\rm GW}(f)}{2\pi^2 f^2}}, \tag{4.14}$$

where $\mathcal{H}_0 \approx 68$ km/s/Mpc is today's Hubble rate. We compare the results with the spectral slope $\beta = d\log h_c(f)/d\log f$ modeling the NANOGrav strain spectrum with a simple power law of the form $h_c(f) = A_{\rm GW}(f/f_{\rm PTA})^\beta$. Expressing β in terms of another parameter $\gamma_{\rm GW} = 3 - 2\beta$, the 1σ fit to NANOGrav 15-yr data gives $\gamma_{\rm GW} \simeq 3.2 \pm 0.6$ around $f \sim 1/(10\text{yr})$ [1]. This favorable range is shown with gray bands superimposed on our strain plot. We find that the spectral tilt of the phase transition signal is in tension in some range of the frequency band probed by NANOGrav.

5 Final remarks

Here we want to draw some final remarks on the results we obtained and how these can be further extended and improved.

- Our results are compatible with those presented in [64]. The differences can be all understood in terms of the different expression we are using to describe the GW spectrum from sound waves, the Eq. (4.7). This supersedes the expression used in [64] based on [65]. The suppression factor taking into account the shorter duration of the stage of GW production compared to the duration of the phase transition is somehow compensated by the fact that the new expression we are using is extended to higher values of α. However, our description of bubble velocity in terms of Jouguet solutions should be clearly replaced by a more advanced one taking into account friction though we do not expect huge changes. Another important difference is that compared to [65] the peak frequency is more than doubled and this explains why we obtain higher values of $T'_\star \sim 100\,\mathrm{keV}$ for the peak value to be in the nHz range spanned by the NANOGrav signal.

- Our peak amplitude can be at most $h^2\Omega_{\mathrm{gw}}(f) \sim 10^{-11}$ at the NANOGrav frequencies and cannot reproduce the whole NANOGrav signal. However, it can certainly help the contribution from SMBHBs to improve the fit, one of the two options for the presence of new physics suggested by the NANOGrav collaboration analysis. This is sufficient to make greatly interesting our results. Clearly a statistical analysis would be required to find the best fit parameters in our model and to quantify the statistical significance.

- The values $T'_\star \sim 100\,\mathrm{keV}$ that we found in our solutions that enter the NANOGrav frequency range, imply a $\Delta N_\nu^{\mathrm{eff}} \simeq 0.5$ at the time of nucleosynthesis, for $N' = 1$. This is in marginal agreement with the constraint Eq. (3.12) from primordial Deuterium measurements and, therefore, future measurements might be determinant for our solution. On the other hand, the solutions we found can ameliorate the Hubble tension.

- We have not explored the possibility to have $T'_\star \gg 1\,\mathrm{MeV}$ with a massive majoron J' quickly decaying before big bang nucleosynthesis thus avoiding all cosmological constraints. This requires an extension of the model introducing explicit symmetry breaking terms. The introduction of these terms can potentially jeopardise the phase transition as noticed in [64] and for this reason it requires special care.

In conclusion the split majoron model is an appealing possibility to address the NANOGrav signal and it can have connections with many different phenomenologies. It is certainly an example of how the evidence of a GW cosmological background from NANAOGrav are a clear demonstration of how the discovery of GWs have opened a new era in our quest of new physics, that should not too much let us regret for the non-evidence of new physics at the LHC (so far).

Acknowledgments

The authors acknowledge financial support from the STFC Consolidated Grant ST/T000775/1.

References

[1] NANOGrav collaboration, *The NANOGrav 15 yr Data Set: Evidence for a Gravitational-wave Background*, *Astrophys. J. Lett.* **951** (2023) L8 [2306.16213].

[2] NANOGrav collaboration, *The NANOGrav 12.5 yr Data Set: Search for an Isotropic Stochastic Gravitational-wave Background*, *Astrophys. J. Lett.* **905** (2020) L34 [2009.04496].

[3] NANOGrav collaboration, *Searching for Gravitational Waves from Cosmological Phase Transitions with the NANOGrav 12.5-Year Dataset*, Phys. Rev. Lett. **127** (2021) 251302 [2104.13930].

[4] NANOGrav collaboration, *The NANOGrav 15 yr Data Set: Search for Signals from New Physics*, Astrophys. J. Lett. **951** (2023) L11 [2306.16219].

[5] R.w. Hellings and G.s. Downs, *UPPER LIMITS ON THE ISOTROPIC GRAVITATIONAL RADIATION BACKGROUND FROM PULSAR TIMING ANALYSIS*, Astrophys. J. Lett. **265** (1983) L39.

[6] Z. Yi, Q. Gao, Y. Gong, Y. Wang and F. Zhang, *The waveform of the scalar induced gravitational waves in light of Pulsar Timing Array data*, 2307.02467.

[7] Y.-T. Kuang, J.-Z. Zhou, Z. Chang, X. Zhang and Q.-H. Zhu, *Primordial black holes from second order density perturbations as probes of the small-scale primordial power spectrum*, 2307.02067.

[8] D.G. Figueroa, M. Pieroni, A. Ricciardone and P. Simakachorn, *Cosmological Background Interpretation of Pulsar Timing Array Data*, 2307.02399.

[9] C. Unal, A. Papageorgiou and I. Obata, *Axion-Gauge Dynamics During Inflation as the Origin of Pulsar Timing Array Signals and Primordial Black Holes*, 2307.02322.

[10] K.T. Abe and Y. Tada, *Translating nano-Hertz gravitational wave background into primordial perturbations taking account of the cosmological QCD phase transition*, 2307.01653.

[11] G. Cacciapaglia, D.Y. Cheong, A. Deandrea, W. Isnard and S.C. Park, *Composite Hybrid Inflation: Dilaton and Waterfall Pions*, 2307.01852.

[12] L.A. Anchordoqui, I. Antoniadis and D. Lust, *Fuzzy Dark Matter, the Dark Dimension, and the Pulsar Timing Array Signal*, 2307.01100.

[13] S.-P. Li and K.-P. Xie, *A collider test of nano-Hertz gravitational waves from pulsar timing arrays*, 2307.01086.

[14] Y. Xiao, J.M. Yang and Y. Zhang, *Implications of Nano-Hertz Gravitational Waves on Electroweak Phase Transition in the Singlet Dark Matter Model*, 2307.01072.

[15] B.-Q. Lu and C.-W. Chiang, *Nano-Hertz stochastic gravitational wave background from domain wall annihilation*, 2307.00746.

[16] C. Zhang, N. Dai, Q. Gao, Y. Gong, T. Jiang and X. Lu, *Detecting new fundamental fields with Pulsar Timing Arrays*, 2307.01093.

[17] R.A. Konoplya and A. Zhidenko, *Asymptotic tails of massive gravitons in light of pulsar timing array observations*, 2307.01110.

[18] D. Chowdhury, G. Tasinato and I. Zavala, *Dark energy, D-branes, and Pulsar Timing Arrays*, 2307.01188.

[19] X. Niu and M.H. Rahat, *NANOGrav signal from axion inflation*, 2307.01192.

[20] L. Liu, Z.-C. Chen and Q.-G. Huang, *Implications for the non-Gaussianity of curvature perturbation from pulsar timing arrays*, 2307.01102.

[21] J.R. Westernacher-Schneider, J. Zrake, A. MacFadyen and Z. Haiman, *Characteristic signatures of accreting binary black holes produced by eccentric minidisks*, 2307.01154.

[22] Y. Gouttenoire, S. Trifinopoulos, G. Valogiannis and M. Vanvlasselaer, *Scrutinizing the Primordial Black Holes Interpretation of PTA Gravitational Waves and JWST Early Galaxies*, 2307.01457.

[23] T. Ghosh, A. Ghoshal, H.-K. Guo, F. Hajkarim, S.F. King, K. Sinha et al., *Did we hear the sound of the Universe boiling? Analysis using the full fluid velocity profiles and NANOGrav 15-year data*, 2307.02259.

[24] S. Datta, *Inflationary gravitational waves, pulsar timing data and low-scale-leptogenesis*, 2307.00646.

[25] D. Borah, S. Jyoti Das and R. Samanta, *Inflationary origin of gravitational waves with \textitMiracle-less WIMP dark matter in the light of recent PTA results*, 2307.00537.

[26] B. Barman, D. Borah, S. Jyoti Das and I. Saha, *Scale of Dirac leptogenesis and left-right symmetry in the light of recent PTA results*, 2307.00656.

[27] Y.-C. Bi, Y.-M. Wu, Z.-C. Chen and Q.-G. Huang, *Implications for the Supermassive Black Hole Binaries from the NANOGrav 15-year Data Set*, 2307.00722.

[28] S. Wang, Z.-C. Zhao, J.-P. Li and Q.-H. Zhu, *Exploring the Implications of 2023 Pulsar Timing Array Datasets for Scalar-Induced Gravitational Waves and Primordial Black Holes*, 2307.00572.

[29] T. Broadhurst, C. Chen, T. Liu and K.-F. Zheng, *Binary Supermassive Black Holes Orbiting Dark Matter Solitons: From the Dual AGN in UGC4211 to NanoHertz Gravitational Waves*, 2306.17821.

[30] A. Yang, J. Ma, S. Jiang and F.P. Huang, *Implication of nano-Hertz stochastic gravitational wave on dynamical dark matter through a first-order phase transition*, 2306.17827.

[31] A. Eichhorn, R.R. Lino dos Santos and J.a.L. Miqueleto, *From quantum gravity to gravitational waves through cosmic strings*, 2306.17718.

[32] H.-L. Huang, Y. Cai, J.-Q. Jiang, J. Zhang and Y.-S. Piao, *Supermassive primordial black holes in multiverse: for nano-Hertz gravitational wave and high-redshift JWST galaxies*, 2306.17577.

[33] Y. Gouttenoire and E. Vitagliano, *Domain wall interpretation of the PTA signal confronting black hole overproduction*, 2306.17841.

[34] Y.-F. Cai, X.-C. He, X. Ma, S.-F. Yan and G.-W. Yuan, *Limits on scalar-induced gravitational waves from the stochastic background by pulsar timing array observations*, 2306.17822.

[35] K. Inomata, K. Kohri and T. Terada, *The Detected Stochastic Gravitational Waves and Sub-Solar Primordial Black Holes*, 2306.17834.

[36] G. Lazarides, R. Maji and Q. Shafi, *Superheavy quasi-stable strings and walls bounded by strings in the light of NANOGrav 15 year data*, 2306.17788.

[37] P.F. Depta, K. Schmidt-Hoberg and C. Tasillo, *Do pulsar timing arrays observe merging primordial black holes?*, 2306.17836.

[38] S. Blasi, A. Mariotti, A. Rase and A. Sevrin, *Axionic domain walls at Pulsar Timing Arrays: QCD bias and particle friction*, 2306.17830.

[39] L. Bian, S. Ge, J. Shu, B. Wang, X.-Y. Yang and J. Zong, *Gravitational wave sources for Pulsar Timing Arrays*, 2307.02376.

[40] G. Franciolini, D. Racco and F. Rompineve, *Footprints of the QCD Crossover on Cosmological Gravitational Waves at Pulsar Timing Arrays*, 2306.17136.

[41] Z.-Q. Shen, G.-W. Yuan, Y.-Y. Wang and Y.-Z. Wang, *Dark Matter Spike surrounding Supermassive Black Holes Binary and the nanohertz Stochastic Gravitational Wave Background*, 2306.17143.

[42] G. Lambiase, L. Mastrototaro and L. Visinelli, *Astrophysical neutrino oscillations after pulsar timing array analyses*, 2306.16977.

[43] C. Han, K.-P. Xie, J.M. Yang and M. Zhang, *Self-interacting dark matter implied by nano-Hertz gravitational waves*, 2306.16966.

[44] S.-Y. Guo, M. Khlopov, X. Liu, L. Wu, Y. Wu and B. Zhu, *Footprints of Axion-Like Particle in Pulsar Timing Array Data and JWST Observations*, 2306.17022.

[45] Z. Wang, L. Lei, H. Jiao, L. Feng and Y.-Z. Fan, *The nanohertz stochastic gravitational-wave background from cosmic string Loops and the abundant high redshift massive galaxies*, 2306.17150.

[46] J. Ellis, M. Lewicki, C. Lin and V. Vaskonen, *Cosmic Superstrings Revisited in Light of NANOGrav 15-Year Data*, 2306.17147.

[47] S. Vagnozzi, *Inflationary interpretation of the stochastic gravitational wave background signal detected by pulsar timing array experiments*, 2306.16912.

[48] K. Fujikura, S. Girmohanta, Y. Nakai and M. Suzuki, *NANOGrav Signal from a Dark Conformal Phase Transition*, 2306.17086.

[49] N. Kitajima, J. Lee, K. Murai, F. Takahashi and W. Yin, *Nanohertz Gravitational Waves from Axion Domain Walls Coupled to QCD*, 2306.17146.

[50] G. Franciolini, A. Iovino, Junior., V. Vaskonen and H. Veermae, *The recent gravitational wave observation by pulsar timing arrays and primordial black holes: the importance of non-gaussianities*, 2306.17149.

[51] E. Megias, G. Nardini and M. Quiros, *Pulsar Timing Array Stochastic Background from light Kaluza-Klein resonances*, 2306.17071.

[52] J. Ellis, M. Fairbairn, G. Hütsi, J. Raidal, J. Urrutia, V. Vaskonen et al., *Gravitational Waves from SMBH Binaries in Light of the NANOGrav 15-Year Data*, 2306.17021.

[53] Y. Bai, T.-K. Chen and M. Korwar, *QCD-Collapsed Domain Walls: QCD Phase Transition and Gravitational Wave Spectroscopy*, 2306.17160.

[54] J. Yang, N. Xie and F.P. Huang, *Nano-Hertz stochastic gravitational wave background as hints of ultralight axion particles*, 2306.17113.

[55] A. Ghoshal and A. Strumia, *Probing the Dark Matter density with gravitational waves from super-massive binary black holes*, 2306.17158.

[56] H. Deng, B. Bécsy, X. Siemens, N.J. Cornish and D.R. Madison, *Searching for gravitational wave burst in PTA data with piecewise linear functions*, 2306.17130.

[57] P. Athron, A. Fowlie, C.-T. Lu, L. Morris, L. Wu, Y. Wu et al., *Can Supercooled Phase Transitions explain the Gravitational Wave Background observed by Pulsar Timing Arrays?*, 2306.17239.

[58] A. Addazi, Y.-F. Cai, A. Marciano and L. Visinelli, *Have pulsar timing array methods detected a cosmological phase transition?*, 2306.17205.

[59] V.K. Oikonomou, *Flat Energy Spectrum of Primordial Gravitational Waves vs Peaks and the NANOGrav 2023 Observation*, 2306.17351.

[60] N. Kitajima and K. Nakayama, *Nanohertz gravitational waves from cosmic strings and dark photon dark matter*, 2306.17390.

[61] A. Mitridate, D. Wright, R. von Eckardstein, T. Schröder, J. Nay, K. Olum et al., *PTArcade*, 2306.16377.

[62] S.F. King, D. Marfatia and M.H. Rahat, *Towards distinguishing Dirac from Majorana neutrino mass with gravitational waves*, 2306.05389.

[63] J. Liu, *Distinguishing nanohertz gravitational wave sources through the observations of ultracompact minihalos*, 2305.15100.

[64] P. Di Bari, D. Marfatia and Y.-L. Zhou, *Gravitational waves from first-order phase transitions in Majoron models of neutrino mass*, *JHEP* **10** (2021) 193 [2106.00025].

[65] C. Caprini et al., *Science with the space-based interferometer eLISA. II: Gravitational waves from cosmological phase transitions*, *JCAP* **04** (2016) 001 [1512.06239].

[66] P. Di Bari, S.F. King and M.H. Rahat, *Gravitational waves from phase transitions and cosmic strings in neutrino mass models with multiple Majorons*, 2306.04680.

[67] Y. Chikashige, R.N. Mohapatra and R.D. Peccei, *Are There Real Goldstone Bosons Associated with Broken Lepton Number?*, *Phys. Lett. B* **98** (1981) 265.

[68] P. Di Bari, *Cosmology and the early Universe*, Series in Astronomy and Astrophysics, CRC Press (5, 2018).

[69] B.D. Fields, K.A. Olive, T.-H. Yeh and C. Young, *Big-Bang Nucleosynthesis after Planck*, *JCAP* **03** (2020) 010 [1912.01132].

[70] Planck collaboration, *Planck 2018 results. VI. Cosmological parameters*, *Astron. Astrophys.* **641** (2020) A6 [1807.06209].

[71] Z. Chacko, L.J. Hall, T. Okui and S.J. Oliver, *CMB signals of neutrino mass generation*, *Phys. Rev. D* **70** (2004) 085008 [hep-ph/0312267].

[72] M. Escudero and S.J. Witte, *A CMB search for the neutrino mass mechanism and its relation to the Hubble tension*, *Eur. Phys. J. C* **80** (2020) 294 [1909.04044].

[73] M. Escudero and S.J. Witte, *The hubble tension as a hint of leptogenesis and neutrino mass generation*, *Eur. Phys. J. C* **81** (2021) 515 [2103.03249].

[74] N. Blinov and G. Marques-Tavares, *Interacting radiation after Planck and its implications for the Hubble Tension*, *JCAP* **09** (2020) 029 [2003.08387].

[75] S. Sandner, M. Escudero and S.J. Witte, *Precision CMB constraints on eV-scale bosons coupled to neutrinos*, 2305.01692.

[76] M. Hindmarsh, S.J. Huber, K. Rummukainen and D.J. Weir, *Shape of the acoustic gravitational wave power spectrum from a first order phase transition*, *Phys. Rev. D* **96** (2017) 103520 [1704.05871].

[77] D.J. Weir, *Gravitational waves from a first order electroweak phase transition: a brief review*, *Phil. Trans. Roy. Soc. Lond. A* **376** (2018) 20170126 [1705.01783].

[78] P.J. Steinhardt, *Relativistic Detonation Waves and Bubble Growth in False Vacuum Decay*, *Phys. Rev. D* **25** (1982) 2074.

[79] J.R. Espinosa, T. Konstandin, J.M. No and G. Servant, *Energy Budget of Cosmological First-order Phase Transitions*, *JCAP* **06** (2010) 028 [1004.4187].

[80] D. Cutting, M. Hindmarsh and D.J. Weir, *Vorticity, kinetic energy, and suppressed gravitational wave production in strong first order phase transitions*, *Phys. Rev. Lett.* **125** (2020) 021302 [1906.00480].

[81] J. Ellis, M. Lewicki and J.M. No, *On the Maximal Strength of a First-Order Electroweak Phase Transition and its Gravitational Wave Signal*, *JCAP* **04** (2019) 003 [1809.08242].

[82] H.-K. Guo, K. Sinha, D. Vagie and G. White, *Phase Transitions in an Expanding Universe: Stochastic Gravitational Waves in Standard and Non-Standard Histories*, *JCAP* **01** (2021) 001 [2007.08537].